



**HAL**  
open science

## Synthesis of isoprene-based triblock copolymers by nitroxide-mediated polymerization

Adrien Métafiot, Sébastien Pruvost, Jean-François Gérard, Brigitte Defoort,  
Milan Marić

► **To cite this version:**

Adrien Métafiot, Sébastien Pruvost, Jean-François Gérard, Brigitte Defoort, Milan Marić. Synthesis of isoprene-based triblock copolymers by nitroxide-mediated polymerization. *European Polymer Journal*, 2020, 134, pp.109798 -. 10.1016/j.eurpolymj.2020.109798 . hal-03490769

**HAL Id: hal-03490769**

**<https://hal.science/hal-03490769>**

Submitted on 3 Jun 2022

**HAL** is a multi-disciplinary open access archive for the deposit and dissemination of scientific research documents, whether they are published or not. The documents may come from teaching and research institutions in France or abroad, or from public or private research centers.

L'archive ouverte pluridisciplinaire **HAL**, est destinée au dépôt et à la diffusion de documents scientifiques de niveau recherche, publiés ou non, émanant des établissements d'enseignement et de recherche français ou étrangers, des laboratoires publics ou privés.



Distributed under a Creative Commons Attribution - NonCommercial 4.0 International License

# Synthesis of Isoprene-based Triblock Copolymers by Nitroxide-Mediated Polymerization

Adrien Métafiot,<sup>1,2,3\*</sup> Sébastien Pruvost,<sup>2</sup> Jean-François Gérard,<sup>2</sup> Brigitte Defoort,<sup>3</sup> and Milan Marić<sup>1</sup>

<sup>1</sup>Department of Chemical Engineering, McGill University, 3610 University St., Montreal, H3A 0C5 Quebec, Canada

<sup>2</sup>Ingénierie des Matériaux Polymères (IMP), CNRS UMR5223, INSA – Lyon, 17 Jean Capelle Avenue, 69621 Villeurbanne, France

<sup>3</sup>ArianeGroup, Avenue du Général Niox, 33160 Saint-Médard-en-Jalles, France

\*Corresponding author

**Keywords:** isoprene; styrene; isobornyl methacrylate; nitroxide-mediated polymerization; block copolymers;

**Abstract:** The nitroxide-mediated polymerization (NMP) of isoprene (I) initiated by the poly(ethylene-*stat*-butylene)-(SG1)<sub>2</sub> dialkoxyamine (PEB-(SG1)<sub>2</sub>) at 115 °C in 50 vol% pyridine led to *cis*-1,4-rich poly(isoprene)s (PIs), exhibiting  $M_{n, GPC} = 52$ -59K (PI equivalents) and  $\bar{D} = 1.46$ -1.59. S-I-S triblock copolymers (S = styrene,  $M_{n, GPC} = 95$ -109K,  $\bar{D} = 2.11$ -2.29,  $F_S = 0.30$ -0.49) were synthesized via subsequent S chain-extensions in bulk at 115 °C from these PI-(SG1)<sub>2</sub> macro-initiators. A micro-phase separation, exhibiting possibly a cylindrical or lamellar morphology, was observed by atomic force microscopy for a S-I-S having  $F_S = 0.30$ . Tensile strength at break  $\sigma_B = 2.8$ -4.1 MPa and elongation at break  $\varepsilon_B \sim 375$ -450 % were measured for S-I-S samples with  $F_S = 0.30$ -0.38. The substitution of the PS outer segments by more rigid segments rich in isobornyl methacrylate (IBOMA) units allowed to improve the stress-strain properties, with  $\sigma_B = 11.4 \pm 0.6$  MPa and  $\varepsilon_B = 1356 \pm 214$  %. This IBOMA-I-IBOMA type copolymer also displayed an upper service temperature greater than 150 °C.

**Introduction:** Styrenic block copolymers (SBCs) are a class of thermoplastic elastomers (TPEs). They can be defined as simple C-A-C triblock copolymers where A is an elastomeric segment, typically poly(isoprene) (PI) or poly(butadiene) (PB), and C is a poly(styrene) (PS) or poly(styrene)-derivative segment. Due to the structural incompatibility between the undiluted and amorphous soft and hard blocks, these copolymers form two separated phases in bulk at ambient conditions: the rigid domain imparting the strength and the flexible domain imparting elastomeric characteristics to the material. The hard phase is typically present in a minority and consists of separate regions from which the glassy domains are attached to the ends of the elastomeric chains and create physical junction points similar to chemical crosslinks. The elastomeric mid-segments are tied together in a three-dimensional network. Accordingly, these triblock thermoplastics behave, at room temperature, in many ways like vulcanized rubbers. Above the glass transition temperature of the hard blocks, these latter components soften, and the material becomes a viscous fluid. The block copolymer chains are no longer locked into position and all the chains are free to flow. The softening of the hard domains, when increasing the temperature, reduces drastically the stress-strain properties of the material, which exhibits thus a limited upper service temperature. However, it also offers a major advantage in comparison to vulcanized rubbers: processing, joining or shaping can be done using standard techniques applied for thermoplastics in the melt state [1,2].

Anionic polymerization is the most studied approach for the formation of SBCs and is, to this day, the only technique employed industrially. This ionic method is typically initiated by an organolithium species, such as *sec*-butyllithium, providing a rapid initiation rate, and it proceeds ideally in the absence of chain termination or transfer. Under the appropriate conditions, the anionic polymerization is thus living and can be used for the formation of a variety of block copolymers with prescribed molecular weights, narrow molecular weight distributions, and well-defined block lengths [3]. Applied to SBCs, such a precise control of the structure ensures the neat segregation of the

dissimilar blocks, leading to nanophase-separated morphologies, and thus tensile properties comparable to those of commercial thermoset elastomers [4].

Although anionic polymerization is undoubtedly the most efficient method to produce well-defined block copolymers with generally a very low dispersity ( $\mathcal{D}$ ) of the polymer chains, the experimental conditions are stringent and demanding. Oxygen, water, or any other impurity must be completely eliminated to prevent undesirable reaction of the highly reactive propagating species. Even a concentration at the part per million level of these impurities can markedly affect the polymerization [5]. Moreover, prior to the polymerization, numerous steps are paramount. Degassing mainly oxygen via freeze-thaw cycles, distillation of solvents and monomers, dilution and ampoullization are common procedures when performing ionic polymerization [6,7]. Therefore, it is of interest to explore a way of producing high-value SBCs under simpler and perhaps less costly experimental conditions.

The development of several controlled radical systems during the last couple of decades, termed reversible-deactivation radical polymerizations (RDRPs) [8-12], utilizing an intermittent formation of active propagating species, has approached many of the features in ionic polymerization systems. Among the various RDRP methods, nitroxide-mediated controlled radical polymerization (NMP) [10,11,13] is based on a reversible radical mechanism where a stable nitroxide, radical acting as a controlling agent, is reacting with the growing propagating macro-radical to yield a dormant chain. Subsequently, the terminal alkoxyamine group on the dormant chain generates in turn the propagating radical and the stable nitroxide by a homolytic cleavage upon a temperature increase [14].

NMP appears particularly suitable to the preparation of SBCs in a straightforward manner. Indeed, under homogeneous conditions in bulk, NMP can consist solely of a unimolecular initiator and the monomer(s). Efficient monocomponent initiating systems, exhibiting high dissociation constants ( $k_{\text{as}}$ ) and low activation energies ( $E_{\text{as}}$ ), are commercially available such as the 2-(*tert*-butyl[1-(diethoxyphosphoryl)-2,2-dimethylpropyl]aminoxy)-2-methylpropionic acid alkoxyamine called BlocBuilder™ (provided by Arkema) [15,16]. Furthermore, prior to polymerization, monomer purification is only necessary if this latter contains significant concentrations of inhibitor. Last but not least, the well-controlled NMP of conjugated diene monomers, such as butadiene (B) [17,18] and more importantly isoprene (I) [19], was reported since the first reports of NMP by Georges *et al.* and by Boutevin *et al.* using in both cases 2,2,6,6-tetramethylpiperidiny-1-oxyl (TEMPO) [20], a stable free nitroxide. Shortly after, well-defined homopolymers and copolymer architectures based on either B or I were achieved using the 2,2,5-trimethyl-4-phenyl-3-azahexane-3-oxyl nitroxide (TIPNO) [21-25], demonstrating the ability of this controlled radical polymerization of providing poly(diene)s with high degrees of polymerization and low  $\mathcal{D}$ . *N-tert*-butyl-*N*-[1-diethylphosphono-(2,2-dimethylpropyl)] nitroxide (SG1) also demonstrated an excellent ability to control the polymerization of I [26-28].

Recently, we reported the synthesis by NMP of a triblock copolymer based on a flexible poly( $\beta$ -myrcene) P(*My*) mid-segment and two outer rigid segments containing mostly isobornyl methacrylate (IBOMA) units [29]. This IBOMA-*My*-IBOMA type triblock copolymer displayed micro-phase separation due to the immiscibility between P(*My*) and the P(IBOMA)-rich segments. Moreover, it exhibited a tensile strength at break  $\sigma_{\text{B}} \sim 4$  MPa and a tensile elongation at break  $\varepsilon_{\text{B}} \sim 500\%$ . In order to improve the stress-strain properties of this material, the replacement of the soft P(*My*) mid-block by PI is promising. Indeed, a more entangled elastomeric phase of the triblock copolymer can be obtained by incorporating a PI mid-segment, which has much lower entanglement molecular weight ( $M_{\text{e,PI}} = 4\text{-}6$  kg.mol<sup>-1</sup>) compared to that of P(*My*) ( $M_{\text{e,P(My)}} = 22\text{-}31$  kg.mol<sup>-1</sup>) [30].

The aim of the work was to prepare by NMP well-tailored triblock copolymers, composed of an entangled PI mid-segment and two outer and identical hard blocks with high thermal stability and better mechanical properties. For this purpose, isoprene homopolymerization mediated by the SG1 free nitroxide was first studied in order to produce a PI block, exhibiting a relatively high average chain length as well as an active feature (chain ends capped by a SG1 moiety). Then, S and IBOMA chain-extensions from PI were performed and the resulting S-I-S and IBOMA-I-IBOMA type copolymers were characterized via tensile, thermal and rheological tests.

## Experimental

## Materials.

Basic alumina ( $\text{Al}_2\text{O}_3$ , Brockmann, Type I, 150 mesh), calcium hydride ( $\text{CaH}_2$ , 90–95% reagent grade), 2,6-di-*tert*-butyl-4-methylphenol (BHT,  $\geq 99\%$ ), thiophenol (97%), pyridine ( $\geq 99\%$ , ACS reagent) and benzene ( $\geq 99\%$ , ACS reagent) were purchased from Sigma-Aldrich and used as received. Toluene ( $\geq 99\%$ ), methanol ( $\text{MeOH}$ ,  $\geq 99\%$ ), methylene chloride ( $\text{CH}_2\text{Cl}_2$ , 99.9% certified ACS), chloroform ( $\text{CHCl}_3$ , 99.8%), and tetrahydrofuran (THF, 99.9% HPLC grade for GPC characterization) were obtained from Fisher Scientific and used as received. Telechelic poly(ethylene-*stat*-butylene) difunctional initiator PEB-(SG1)<sub>2</sub> terminated with *N-tert*-Butyl-*N*-[1-diethylphosphono-(2,2-dimethylpropyl)] nitroxide (SG1) was produced relying on a published synthesis route [31], from hydroxyl terminated poly(ethylene-*stat*-butylene) (PEB-(OH)<sub>2</sub>, Kraton™ D2203) obtained from Kraton, acryloyl chloride (98%) acquired from Sigma-Aldrich and 2-(*tert*-butyl[1-(diethoxyphosphoryl)-2,2-dimethylpropyl]aminoxy)-2-methylpropionic acid, also known as MAMA SG1 (BlocBuilder-MA™, BB, 99%, provided by Arkema and used without further purification). Isoprene (I, 99%, Sigma-Aldrich), styrene (S, 99%, Fisher Scientific) and isobornyl methacrylate (IBOMA, Visiomer® Terra from Evonik) were purified by passing through a column of basic alumina mixed with 5 wt% calcium hydride and then stored in a sealed flask under a head of nitrogen in a refrigerator until needed. The deuterated chloroform ( $\text{CDCl}_3$ , 99.8%) used as a solvent for nuclear magnetic resonance (NMR) was obtained from Cambridge Isotopes Laboratory.

## Synthesis of PI-(SG1)<sub>2</sub> by NMP.

In a typical procedure (experiment I3, Table 1), PEB-(SG1)<sub>2</sub> ( $0.0024 \text{ mol.L}^{-1}$ ,  $M_{n,\text{GPC}} = 5.7\text{K}$ ) was placed in a 48 mL ChemGlass high-pressure reactor containing a magnetic stir bar and fitted with a plunger valve and a thermowell. Previously purified isoprene ( $4.93 \text{ mol.L}^{-1}$ ) and pyridine ( $6.17 \text{ mol.L}^{-1}$ ) were added and the reactor was subjected to three cycles of freeze-thaw degassing, then backfilled with nitrogen. The reactor was placed in a vigorously stirred oil bath at 115 °C for 11 h and then cooled to room temperature. The contents of the reactor were transferred to a pre-weighed flask and weighed. Unreacted isoprene was removed in the oven under vacuum at 30 °C and the residual poly(isoprene) (PI) and any unreacted PEB-(SG1)<sub>2</sub> (mass neglected) were weighed to calculate isoprene conversion gravimetrically. At the end of the experiment, the gravimetric conversion after 11h of reaction was 17.5%, with  $M_{n,\text{GPC}} = 36.7\text{K}$  (Figure 2a) and a molecular weight distribution  $\mathcal{D} = 1.29$  (Figure 2b), as determined by gel permeation chromatography.

Identical pressure tubes were prepared, degassed and allowed to react for various periods in order to trace the evolution of  $M_{n,\text{GPC}}$ ,  $\mathcal{D}$  and isoprene conversion with time. The exact same procedure was followed for the isoprene polymerization in bulk (experiments I1 and I2, Table 1).

For experiments I4 to I7 (Table 2A), fractionation was performed using a methanol (non-solvent) / benzene (solvent) pair (1 cycle) to remove the low molecular weight species.

## S or IBOMA/S chain-extension from PI-(SG1)<sub>2</sub>.

The chain-extension of the PI-(SG1)<sub>2</sub> macro-initiator with S in bulk is detailed below as an example (experiment S-I4-S, Table 2B, similar protocol for IBOMA/S chain-extension). PI-(SG1)<sub>2</sub> ( $0.004 \text{ mol.L}^{-1}$ ) and previously purified S ( $5.71 \text{ mol.L}^{-1}$ ) were added in a 25-mL three-necked round-bottom glass flask equipped with a condenser, a thermal well and a magnetic Teflon stir bar. The reactor was sealed, vigorous stirring was applied and a purge of ultra-pure nitrogen was then introduced to the reactor for 30 min. The reactor was then heated to 115 °C and allowed to react for 140 min while maintaining a nitrogen purge. The resulting polymer sample ( $M_{n,\text{GPC}} = 96.4\text{K}$ ,  $\mathcal{D} = 2.19$ ) was precipitated in excess methanol and dried under vacuum at 50 °C overnight. Lastly, fractionation was performed using a methanol (non-solvent) / benzene (solvent) pair (1 cycle) to remove the low molecular weight species. The final fractionated triblock polymer S-I4-S exhibited  $M_{n,\text{GPC}} = 103.1\text{K}$ ,  $\mathcal{D} = 2.11$  and a molar composition of S in the final copolymer  $F_S = 0.49$  (Table 2C), as determined by proton nuclear magnetic resonance (<sup>1</sup>H NMR).

## Characterization.

Isoprene conversion was determined by gravimetry and calculated from the following formula:

$$X_I = (m_{r+p} - m_r) / [(m_{r+p+s} - m_r) \times (1 - w_s)] \quad (1)$$

in which  $m_r$  is the mass of the empty reactor,  $m_{r+p+s}$  is the mass of the reactor containing the reaction solution just after the experiment (polymer, unreacted monomer and solvent if used),  $m_{r+p}$  is the mass of the reactor containing only the polymer after drying and  $w_s$  is the mass fraction of solvent relative to the initial masses of initiator and monomer. In order to prevent any overestimation, drying of the samples was performed first under air flow for 24 h and then under vacuum at 50 °C for 24 h to maximize the removal of non-polymer components.

IBOMA and S conversions were determined with a Varian NMR Mercury spectrometer (300 MHz, 32 scans) using  $\text{CDCl}_3$ . The signal of the solvent ( $\delta = 7.27$  ppm) was used as reference for chemical shifts. IBOMA conversion was obtained using the  $^1\text{H}$  NMR peaks of the vinyl protons of the monomer ( $\delta = 6.05$  and  $5.50$  ppm, 2H) and the aromatic proton of both monomer and polymer ( $\delta = 4.65$ - $4.20$  ppm, 1H). S conversion was determined using the vinyl protons of the monomer ( $\delta = 6.80$ - $6.70$ ,  $5.80$ - $5.70$  and  $5.30$ - $5.20$  ppm, 3H) and the aromatic protons of both monomer and polymer ( $\delta = 7.50$ - $6.90$  ppm, 5H). Regarding the regioselectivity of the PI samples, the signal at  $\delta = 4.75$ - $4.55$  ppm of the  $^1\text{H}$  NMR spectra is attributed to olefinic protons of 3,4-addition ( $\text{C}=\text{CH}_2$ ). The peaks detectable at  $5.00$ - $4.80$  ppm and  $5.85$ - $5.65$  ppm correspond to the olefinic protons of 1,2-addition ( $\text{CH}=\text{CH}_2$ ). Moreover, the olefinic protons' signal of *cis*- and *trans*-1,4-addition ( $\text{C}=\text{CH}$ ) are observed at  $\delta = 5.15$ - $5.05$  ppm. The sharp chemical shift from the methyl protons of *cis*-1,4 and *trans*-1,4 units ( $\text{C}-\text{CH}_3$ ) is seen at  $1.67$  and  $1.59$  ppm, respectively [32,33].

The relative number-average molecular weight ( $M_{n,\text{GPC}}$ , dimensionless and defined as being PI equivalents) and the dispersity ( $D = M_{w,\text{GPC}}/M_{n,\text{GPC}}$ ) for each polymer sample was measured using gel permeation chromatography (GPC, Water Breeze, differential refractive index RI 2414 detector, 40 °C) with HPLC grade THF as the mobile phase (flow rate of  $0.3 \text{ mL}\cdot\text{min}^{-1}$ ). The GPC was equipped with 3 Waters Styragel® HR columns (HR1 with a molecular weight measurement range of  $10^2 - 5 \times 10^3 \text{ g}\cdot\text{mol}^{-1}$ , HR2 with a molecular weight measurement range of  $5 \times 10^2 - 2 \times 10^4 \text{ g}\cdot\text{mol}^{-1}$  and HR4 with a molecular weight measurement range of  $5 \times 10^3 - 6 \times 10^5 \text{ g}\cdot\text{mol}^{-1}$ ) and a guard column was used.  $M_{n,\text{GPC}}$  values were determined by calibration with 10 linear narrow molecular weight distribution PI standards (Polymer Standards Service,  $M_n$  ranging from 944 to 951 000  $\text{g}\cdot\text{mol}^{-1}$ ,  $D$  ranging from 1.01 to 1.13).

Thermogravimetric analysis (TGA) was carried out using a Q500TM from TA Instruments under nitrogen or air flow at a ramp rate of  $15 \text{ }^\circ\text{C}\cdot\text{min}^{-1}$ . Samples were heated in aluminum pans. Differential scanning calorimetry (DSC, Q2000TM from TA Instruments) was used under  $\text{N}_2$  atmosphere. Indium was used as a standard to calibrate temperature while heat flow was calibrated via a benzoic acid standard. Three scans per cycle (heat/cool/heat) at a rate of  $10 \text{ }^\circ\text{C}\cdot\text{min}^{-1}$  was set with a temperature range ranging typically from  $-80 \text{ }^\circ\text{C}$  to  $+220 \text{ }^\circ\text{C}$  for the characterization of the triblock copolymers. Only the second heating run was taken into account to eliminate the thermal history. The reported  $T_g$ s were calculated using the inflection method from the change in slope observed in the DSC traces.

The stress-strain features of the triblock copolymers were determined using an MTS Insight material testing system with a 5 kN load cell at room temperature and a cross-head speed of  $15 \text{ mm}\cdot\text{min}^{-1}$ . Dog-bone style tensile specimens (ASTM D638 type V for reference, overall length = 63.5 mm, overall width = 9.53 mm) were prepared by solvent casting. To cast the film, the polymer sample was fully dissolved in dichloromethane ( $\sim 80 \text{ wt}\%$ ) for an hour with continuous stirring using a magnetic stir bar. The solution was cast into a level Teflon Petri dish at room temperature for approximately two days. Then, the drying was completed after placing the film in the oven at  $50 \text{ }^\circ\text{C}$  under vacuum until constant weight was measured. The film samples were cut into typical dog-bone shapes using a sharp blade. Specimens with defects (nicked sides, cracks, air bubbles) on their surface were discarded and were not used in mechanical testing. The samples tested exhibited a mean thickness from  $0.52$  to  $0.65 \text{ mm}$  and a mean width from  $3.10$  to  $3.35 \text{ mm}$ . Each test was considered finished after the complete fracture of the specimen at the narrow section (films that broke near the grips were discarded). More than 3 samples were tested for each batch, and averaged results were

reported using TestWorks 4 software. The Young's modulus was determined as the slope of the stress-strain curve at strains of 0–0.5%.

The mechanical response of the triblock copolymers to torsional oscillation at 0.15 Hz and 1% strain over a typical temperature range of 25 to 240 °C was measured at a rate of 5 °C.min<sup>-1</sup> under N<sub>2</sub> using the CDT 450 convection heated measuring chamber mounted on the Anton Paar Modular Compact Rheometer MCR302. The solid rectangular fixture (SFR) was used, consisting of an upper and a lower holder with insets. Rectangular bars (thickness = 1.02 ± 0.09 mm; width = 8.98 ± 0.18 mm; length = 44.13 ± 0.21) were made by solvent casting, following the above protocol used for preparing the tensile bars. Prior to the torsion tests, dynamic amplitude sweeps at 0.15 Hz and varying strain from 0.01 to 10% were conducted at various temperatures to ensure the material was kept within the linear viscoelastic regime (Supporting Information, Figure S7 for the sample I7-(IBOMA/S)<sub>2</sub>). It should be noted that before the rheological characterization, the removal of the SG1 groups of the sample chain-ends was performed as described elsewhere [34,35].

The micro-phase behavior of the triblock polymers was studied by atomic force microscopy (AFM). AFM images were collected in tapping mode using an AFM Bruker Multimode 8 equipped with Nanoscope V controller. The scanning speed for image acquisition was 0.5 Hz. The used cantilevers are Bruker TAP 300A with a radius of curvature of the tip of 8 nm. Data analyses were processed using the Nanoscope Analysis software (version 1.5). The samples were prepared as follows: the polymer (~ 0.5 g) was fully dissolved in chloroform (~ 10 mL) and one or two drops was spin coated on a silicon wafer, previously rinsed with acetone and cleaned by UV-O<sub>3</sub> for 30 min. Lastly, the coated film was dried at 50 °C under vacuum overnight.

## Results and Discussion

### ■ Preparation of SG1-terminated poly(isoprene) PI-(SG1)<sub>2</sub>

It was first aimed to synthesize by NMP a relatively high  $M_n$  PI telechelic mid-segment, having a high degree of chain-end fidelity at both chain ends. This way, a well-defined poly(diene) exhibiting an elevated entanglement density could be used for the subsequent chain-extensions. Harrisson *et al.* studied the NMP of isoprene in bulk initiated by various SG1-based alkoxyamines [27]. They showed that a good control of the isoprene homopolymerization can be obtained at 115 °C without using additional SG1. Even though the theoretical average molecular weight target was low for each reaction ( $M_{n,target} < 14 \text{ kg.mol}^{-1}$  at quantitative conversion), the resulting PIs exhibited  $\mathcal{D} \leq 1.20$  at the end of the experiments and  $M_{n,s} = 2\text{-}8 \text{ kg.mol}^{-1}$ , slightly below the theoretical ones. This study highlighted the efficiency of the labile second-generation initiators based on SG1 to control isoprene polymerization, notably due to their facile C-ON bond homolysis [36].

In order to prepare a PI macro-initiator terminated by a nitroxide unit at each chain end, it was thus decided to rely on a SG1-based unimolecular dialkoxyamine. Accordingly, a telechelic poly(ethylene-*stat*-butylene) copolymer terminated with SG1 groups and abbreviated as PEB-(SG1)<sub>2</sub> ( $M_{n,GPC} = 5.8\text{K}$  defined as PI equivalents,  $\mathcal{D} = 1.15$ , structure in Figure 1) was synthesized according to the method reported by Lessard *et al* [31]. PEB-(SG1)<sub>2</sub> showed previously its effectiveness to mediate the NMP of  $\beta$ -myrcene, another conjugated 1,3-diene, in bulk at 120 °C [29]. 87 mol% of the PEB-(SG1)<sub>2</sub> terminal groups were SG1 moieties, as characterized by <sup>1</sup>H NMR, allowing to infer the presence of monofunctional and inactive PEB chains. 115 °C was selected as the reaction temperature since it was shown to provide a controlled isoprene polymerization at a decent polymerization rate [27]. Lastly, a high target number-average molecular weight at quantitative conversion ( $M_{n,theo} = 139\text{-}146 \text{ kg.mol}^{-1}$  at  $X_1 = 100\%$ ) was chosen in order to produce relatively long PI chains. The experimental conditions of the isoprene polymerizations performed are summarized in Table 1.

Two first experiments (I1, from 2 to 8h, and I2, from 11 to 17h, Table 1) were conducted in bulk since it corresponds to the easiest system to study, consisting only of purified isoprene (~ 10 mol.L<sup>-1</sup>) and the mono-component PEB-(SG1)<sub>2</sub> initiating system (~ 0.005 mol.L<sup>-1</sup>). The kinetic results are illustrated in Figure 2, which indicated two marked regimes. At a moderate isoprene conversion  $X_1 < 30\%$  (experiment I1), a good control of the polymerization was observed with low dispersity values

( $\bar{D} < 1.26$ , Figure 2b) and experimental  $M_{n,GPC}$ s close to the predicted ones (Figure 2a, GPC calibration curve made with linear PI standards). The rapid dissociation of the dialkoxyamine, resulting in a high concentration of free nitroxide at the early stages of the polymerization, can explain these conclusive results. The negligible contribution of non-reversible termination reactions was also confirmed by the linear trend of  $\ln((1-X_I)^{-1})$  versus time for  $X_I < 30\%$  (Supporting Information, Figure S1, experiment I1), indicating a quasi-constant concentration of the active propagating species. Nonetheless, at  $X_I > 30\%$  (experiment I2, reaction time  $t = 15-17$  h), a clear loss of control was seen with significant deviations of the experimental  $M_{n,GPC}$  values from the predicted line (Figure 2a) and broader molecular weight distributions ( $\bar{D} \geq 1.73$ , Figure 2b). Three reasons can explain this marked loss of control: the high isoprene conversion, e. g. the low isoprene concentration in the medium, favoring self-termination and H-transfer side-reaction between SG1 and the propagating macro-radical; the elevated  $[I]_0 / [PEB-(SG1)_2]_0$  ratio at the commencement of the reaction, increasing the occurrence of chain-transfer reactions to I or PI; the high viscosity of the polymerization at  $X_I > 30\%$ , leading to diffusional limitations [37] and decreasing the probability of the active chain ends to be deactivated by the controlling nitroxide. Therefore, it was decided to perform the polymerization in solution to prevent a significant increase of the viscosity after the early stages of the reaction.

Harrison and coworkers reported an enhanced control over the SG1-based NMP of isoprene in pyridine compared to the same reaction in bulk [28]. Lower  $\bar{D}$  values were obtained, which can be likely caused by the stabilization of the polar SG1 free nitroxide as well as the disruption of intramolecular hydrogen bonding due to the presence of pyridine. Therefore, a third experiment was performed for 25h with the initial addition of 50 vol% pyridine relative to isoprene (experiment I3, Table 1, synthesis route shown in Figure 1).  $M_{n,GPC}$ , from 36.7 to 63K (PI equivalents), increased linearly with conversion and followed closely the theoretical line (Figure 2a). A broadening of the molecular weight distribution was observed with conversion ( $\bar{D} \geq 1.57$  at  $X_I \geq 27\%$ , Figure 2b). In addition to the irreversible terminations occurring during NMP, it may be assumed that the use of PEB-(SG1)<sub>2</sub> as initiator ( $\bar{D} = 1.15$ ), having some monofunctional and/or dead chains, contributed to these high  $\bar{D}$  values. However, it is of interest to note that these conditions allowed the synthesis of a PI sample having a relatively high  $M_{n,GPC} \sim 55K$  with  $\bar{D} \sim 1.55$ , as it can be seen in Figure 2 at  $X_I = 25-30\%$  (reaction time  $t \sim 15h$ ). Consequently, it was decided to synthesize the PI-(SG1)<sub>2</sub> mid-segment by relying on the following experimental conditions: initiation of I with PEB-(SG1)<sub>2</sub> at 115 °C in 50 v% pyridine for about 14-17h and targeting  $M_{n,theo} \sim 145 \text{ kg}\cdot\text{mol}^{-1}$  at quantitative conversion. Four PI macro-initiators (I4 to I7, Table 2A) were synthesized this way and subsequently fractionated (one cycle of benzene/ methanol fractional precipitation) [38,39] to eliminate the shorter chains, the majority of those being presumably irreversibly terminated (not capped by a SG1 unit). The molecular features of the final PI macro-initiators are given in Table 2A.

I4-I7 samples exhibited  $M_{n,GPC}$ s higher than initially predicted ( $M_{n,GPC,I} / M_{n,theo,XI} > 1$ , Table 2A), which can likely be attributed to the incomplete initiator efficiency since only 87 mol% of the PEB-(SG1)<sub>2</sub> chain ends are terminated by SG1 as well as the fractionation of the PIs at the end of the experiments. The selectivity of the PIs produced, containing fractions of 1,4-addition  $> 83 \text{ mol}\%$  and *cis*-1,4-addition  $> 68 \text{ mol}\%$ , was elucidated by <sup>1</sup>H NMR (<sup>1</sup>H NMR spectrum of I4 sample in Supporting Information, Figure S2). Thermal analysis was also used to investigate the physical properties of the NMP-based PIs as a function of temperature. A distinct baseline shift at around  $-60$  °C was observed by DSC for I4 (Supporting Information, Figure S3a), corresponding to its subzero  $T_g$  [40]. The maximum decomposition temperature ( $T_{dec,max}$ , temperature at which weight loss is most apparent) of I4 under air and nitrogen atmospheres was determined via TGA (Supporting Information, Figure S3b) as well. I4 showed a single degradation peak at  $T_{dec,max} = 389$  °C under N<sub>2</sub> flow. The thermal stability of I4 was reduced under air with  $T_{dec,max} = 361$  °C, highlighting the likely occurrence of oxidation reactions which generate chain scissions.

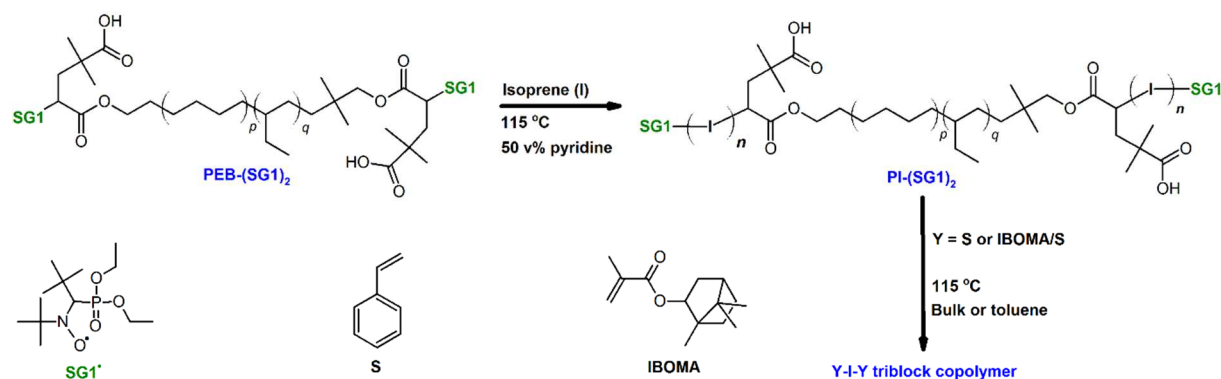


**Figure 1.** Optimized synthesis of PI-(SG1)<sub>2</sub> from PEB-(SG1)<sub>2</sub> difunctional initiator ( $n \gg p, q$ ) at 115 °C in 50 v% pyridine and subsequent chain-extension in bulk or toluene at 115 °C with S or a IBOMA/S mixture. The structures of the SG1\* free nitroxide and S and IBOMA monomers are also depicted. (2-column fitting image)

**Table 1.** Formulations for isoprene polymerizations performed in bulk or in pyridine at T = 115 °C, initiated by PEB-(SG1)<sub>2</sub> and targeting  $M_{n,theo} = 139$ -146 kg.mol<sup>-1</sup> at  $X_I = 100\%$ .

ID	[PEB-(SG1) <sub>2</sub> ] (M)	[I] (M)	Medium	[Solvent] (M)	$M_{n,theo}^{(a)}$ (kg.mol <sup>-1</sup> )	T (°C)	$t^{(b)}$ (h)
I1	0.0051	9.97	Bulk	-	139	115	8
I2	0.0050	10.21	Bulk	-	145	115	17
I3	0.0024	4.93	Pyridine	6.17	146	115	25

a) Rounded values including the number-average molecular weight of PEB-(SG1)<sub>2</sub> ( $M_{n,PEB(SG1)_2} = 5.7K$ ).

b) Samples periodically taken at: 2h, 4h, 6h and 8h (I1); 11h, 13h, 15h and 17h (I2); 11h, 13h, 16h, 19h and 25h (I3).

(2-column fitting image)

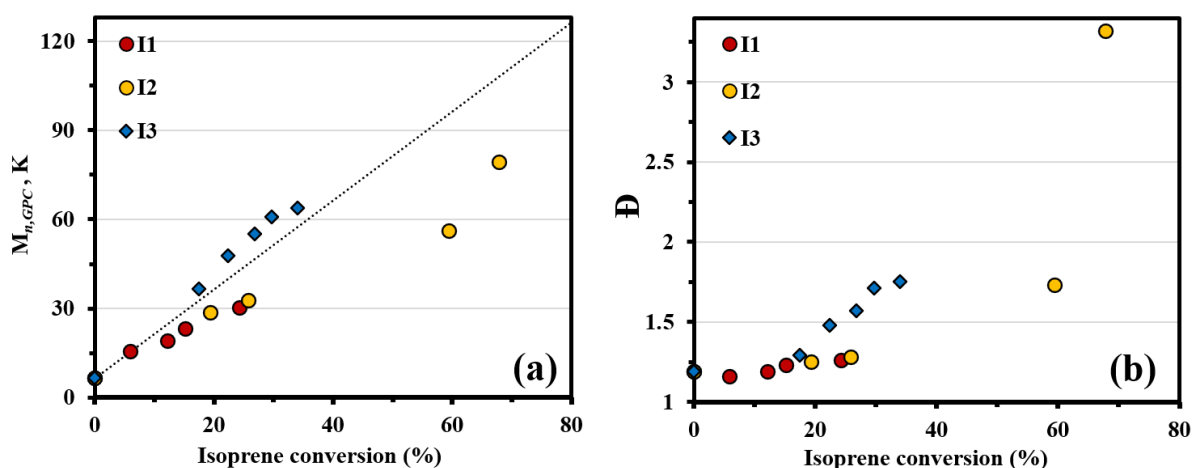


**Figure 2.** (a)  $M_{n,GPC}$  (PI equivalents) versus isoprene conversion  $X_I$  and (b)  $D$  versus  $X_I$  for the isoprene homopolymerizations performed in bulk (experiments I1 and I2) and in pyridine (experiment I3) at 115 °C and initiated by PEB-(SG1)<sub>2</sub>. The dotted black line indicates the theoretical  $M_n$  versus overall conversion based on the monomer to initiator ratio ( $M_{n,theo} \sim 145$  kg.mol<sup>-1</sup> at  $X_I = 100\%$  for

every experiment). All experimental ID are listed in Table 1. (1-column fitting image, top-down organization for (a) and (b))

**Table 2.** Chain-extension of (A) PI-(SG1)<sub>2</sub> macro-initiator with (B) S or IBOMA/S mixture at 115 °C in bulk or in 50 wt% toluene and (C) characteristics of the resulting triblock copolymer.

<b>(A) PI-(SG1)<sub>2</sub> Macro-initiator</b>							
ID	<i>t</i> (h)	<i>X</i> <sub>1</sub> <sup>(a)</sup> (%)	<i>M</i> <sub>n,GPC,1</sub> <sup>(b)</sup> , K	<i>M</i> <sub>n,theo,<i>X</i><sub>1</sub></sub> <sup>(c)</sup> (kg.mol <sup>-1</sup> )	<i>D</i> <sub>1</sub> <sup>(b)</sup>	1,4- <sup>(d)</sup> (mol%)	<i>cis</i> -1,4- <sup>(d)</sup> (mol%)
<b>I4</b>	14	27.2	52.3	46.1	1.47	86.0	71.4
<b>I5</b>	16	29.9	57.8	49.5	1.59	83.7	75.0
<b>I6</b>	17	31.5	59.0	52.2	1.57	84.1	68.8
<b>I7</b>	14	26.0	52.1	44.0	1.46	89.3	72.4
<b>(B) Chain-extension from PI-(SG1)<sub>2</sub></b>							
ID	[PI-(SG1) <sub>2</sub> ] (M)	[S] (M)	[IBOMA] (M)	[Toluene] (M)	<i>M</i> <sub>n,theo,CE</sub> <sup>(e)</sup> (kg.mol <sup>-1</sup> )	T (°C)	<i>t</i> (min)
<b>S-I4-S</b>	0.004	5.71	-	-	201	115	140
<b>S-I5-S</b>	0.003	4.15	-	-	202	115	50
<b>S-I6-S</b>	0.004	6.28	-	-	223	115	80
<b>I7-(IBOMA/S)<sub>2</sub></b>	0.004	0.15	1.57	4.63	143	115	90
<b>(C) Chain-extended triblock copolymer</b>							
ID	<i>X</i> <sub>overall</sub> <sup>(f)</sup> (mol%)	<i>F</i> <sub>S</sub> <sup>(g)</sup>	<i>F</i> <sub>IBOMA</sub> <sup>(g)</sup>	<i>M</i> <sub>n,GPC,2</sub> <sup>(b)</sup> , K	<i>D</i> <sub>2</sub> <sup>(b)</sup>		
<b>S-I4-S</b>	44.1	0.49	-	103.1	2.11		
<b>S-I5-S</b>	31.2	0.30	-	94.6	2.29		
<b>S-I6-S</b>	36.8	0.38	-	109.4	2.18		
<b>I7-(IBOMA/S)<sub>2</sub></b>	57.8	0.06	0.35	94.0	1.76		

a) Isoprene conversion *X*<sub>1</sub> determined gravimetrically.

b) Relative *M*<sub>n,GPC</sub> and *M*<sub>w,GPC</sub> determined by GPC in THF at 40 °C and calibrated with linear PI standards.

c) Predicted *M*<sub>n</sub> at *X*<sub>1</sub> (measured experimentally) and calculated as follows: *M*<sub>n,theo,*X*<sub>1</sub></sub> = (*X*<sub>1</sub>/100)*M*<sub>n,theo</sub>.

d) Isoprene regio- and stereo-selectivity determined by <sup>1</sup>H NMR in CDCl<sub>3</sub>.

e) Rounded targeted number-average molecular weight of the whole chain-extended triblock copolymer at quantitative overall conversion (*X*<sub>overall</sub> = 100%) including *M*<sub>n,PI-(SG1)<sub>2</sub></sub> = 52.1-59.0K.

f) Average conversion was calculated as follows: *X*<sub>overall</sub> = *X*<sub>a</sub>*f*<sub>a,0</sub> + *X*<sub>b</sub>*f*<sub>b,0</sub> where *f*<sub>a,0</sub> and *f*<sub>b,0</sub> are the initial molar fractions of monomer “a” and monomer “b” respectively and *X*<sub>a</sub> and *X*<sub>b</sub>, determined via <sup>1</sup>H NMR, are the individual conversions of “a” and “b” respectively.

g) Molar fraction of S and IBOMA and in the final triblock copolymer, as determined by <sup>1</sup>H NMR in CDCl<sub>3</sub>.

(2-column fitting image)

## ■ S and IBOMA/S chain-extensions from PI-(SG1)<sub>2</sub>

Ideally, the synthesis of a well-defined PI terminated at each chain end by a SG1 moiety allows the addition of two similar blocks via chain-extension. In order to prepare polymer samples similar to styrenic triblock copolymers having a soft mid-segment and two outer rigid segments, it was decided to chain-extend PI-(SG1)<sub>2</sub> with styrene (S, *T*<sub>g</sub> = 100-110 °C for atactic PS with *M*<sub>n</sub> > 100 kg.mol<sup>-1</sup>) [41] and isobornyl methacrylate (IBOMA, *T*<sub>g,P(IBOMA)</sub> ~ 190 °C) [42]. The structure of these two monomers are given in Figure 1.

Preliminary styrene (2.3-2.8 mol.L<sup>-1</sup>) chain-extensions from NMP-based PI-(SG1)<sub>2</sub> samples (*M*<sub>n,GPC</sub> = 46.8-61.0K, *D* = 1.41-1.58, 0.002-0.003 mol.L<sup>-1</sup>) were performed in 50 wt% toluene (4.8-5.7

mol.L<sup>-1</sup>) at reflux temperature (110-114 °C). Despite successful chain-extensions notably marked by the monomodal shift of the GPC chromatograms to lower elution times, indicating a high level of chain end fidelity, a low fraction of styrene (S) was incorporated with a molar fraction of S in the final copolymer  $F_S = 0.07-0.13$ . For purposes of developing relatively tough triblock copolymers which can be characterized by tensile testing and torsional oscillation, the addition of longer PS segments to the PI macro-initiator was targeted. Accordingly, bulk chain-extensions were considered to push the styrene conversion to higher levels. It should be noted that P(I-*b*-S) block copolymers can be obtained via a solvent-free process. For instance, the anionic bulk polymerization to synthesize isoprene-styrene block copolymers by reactive extrusion using a co-rotating twin-screw extruder was reported [43-45].

The chain-extensions of I4, I5 and I6 macro-initiators synthesized previously (Table 2A) with S were performed in bulk at 115 °C (temperature kept under 120 °C to avoid S auto-initiation) [46], at different reaction times (50-140 min) to prepare S-I-S copolymers with various  $F_S$ . The experimental conditions are given in Table 2B. The mass polymerizations were conclusive since the chain-extended products exhibited significantly higher  $M_{n,GPC} = 95-109K$  with  $F_S = 0.30-0.49$  (Table 2C), compared to those of their parent macro-initiators (52-59K, Table 2A). The GPC traces of the S-I-S triblock copolymers retained generally their monomodal nature, as shown in Figure 3a for the experiment S-I4-S (GPC chromatograms of the chain-extensions S-I5-S and S-I6-S depicted in Supporting Information, Figure S4). However, a marked broadening of the molecular weight distribution was observed for every experiment from  $\mathcal{D} = 1.47-1.59$  for the macro-initiators to  $\mathcal{D} = 2.11-2.29$  for the chain-extended products (Tables 2A and 2C respectively). Two main factors may explain this increase in  $\mathcal{D}$ : the presence of dead chains from the PI macro-initiators, which can be qualitatively observed from the GPC results with the tails of the S-I-S samples (~ 22-24 min of elution) overlapping to some degree with the macro-initiator traces (Figure 3a and Figure S4 in Supporting Information); the bulk conditions (high initial concentration of S to dissolve PI-(SG1)<sub>2</sub>, rapid increase in S conversion and viscosity) bringing about irreversible terminations and chain-transfer reactions [47].

It was then attempted to add two P(IBOMA)-rich end blocks to a PI macro-initiator. Compared to the previous reactions with S, the chain-extension with IBOMA appeared more challenging due to the high equilibrium constant  $K$  typically associated for methacrylate-nitroxide systems and the  $\beta$ -hydrogen transfer from the propagating radical to the nitroxide [48,49]. Therefore, the copolymerization approach was employed herein, consisting of the addition of a small amount of an easy-to-control monomer such as S, lowering drastically the average  $\langle K \rangle$  of the reaction [50]. Furthermore, toluene was used to effectively dissolve the poly(diene) and ensure the homogeneity of the reaction medium. The chain-extension of I7 (Table 2A) with a previously purified IBOMA/S mixture (91/9 mol%) in 50 wt% toluene was thus performed at 115 °C for 90 min (Table 2B, experiment I7-(IBOMA/S)<sub>2</sub>). A monomodal shift in molecular weight as a function of elution time from macro-initiator to final chain-extended copolymer was observed in the GPC chromatograms (Figure 3b), indicating the successful addition of the two IBOMA/S segments. As mentioned previously for the S-I-S samples, a population of low  $M_n$  polymers can be observed at about 21-23 min of elution and corresponds likely to inactive macro-initiator. DOSY NMR experiments could be used to ascertain the presence of dead poly(isoprene) chains in the final product. The resulting I7-(IBOMAS/S)<sub>2</sub> triblock copolymer exhibited after fractionation  $M_{n,GPC} = 94.0K$  and  $\mathcal{D} = 1.76$  (Table 2C) and possessed two outer rigid segments containing 85 and 15 mol% of IBOMA and S units respectively, as characterized by <sup>1</sup>H NMR (<sup>1</sup>H NMR spectrum of the final I7-(IBOMAS/S)<sub>2</sub> sample provided in Supporting Information, Figure S5).

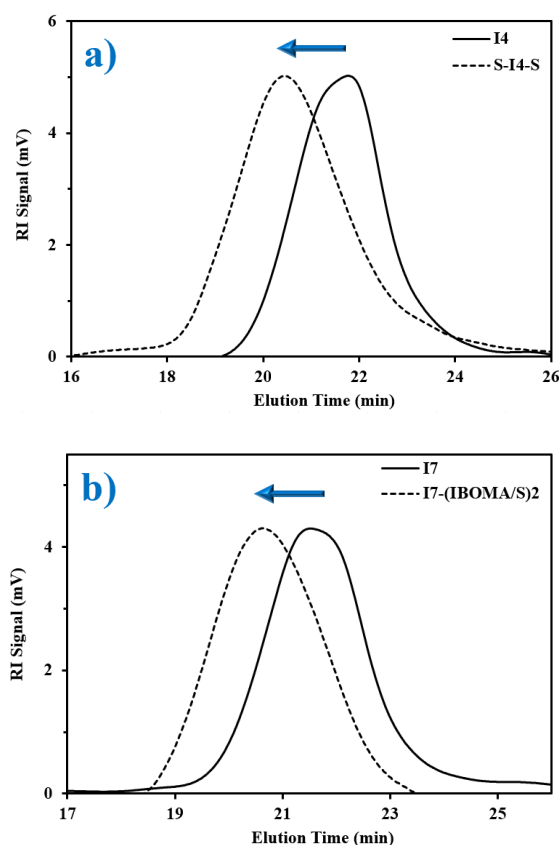


**Figure 3.** Normalized GPC traces for (a) the S chain-extension from I4 in bulk at 115 °C (experiment S-I4-S) and (b) the IBOMA/S chain-extension from I7 in toluene at 115 °C (experiment I7-(IBOMA/S)<sub>2</sub>). (1-column fitting image)

## ■ Characterization of the NMP-based triblock copolymers

### Thermal and dynamic mechanical analyses:

The thermal stability of the copolymer S-I4-S was investigated using thermogravimetric analysis (TGA). A higher maximum decomposition temperature  $T_{\text{dec,max}}$  was determined for this triblock compared to the parent poly(isoprene) I4, whether under nitrogen (+ 31 °C, Figure 4a and Figure S3b in Supporting Information) or under air (+ 37 °C, Figures S6 and S3b in Supporting Information) atmospheres. Such an observation agrees with the higher thermal stability of poly(styrene) ( $T_{\text{dec,max,PS}} = 445$  °C for an atactic PS sample exhibiting  $M_n = 15.6$  kg.mol<sup>-1</sup>) [51], compared to that of poly(diene)s. Under air, the early thermo-oxidative degradation of S-I4-S, starting at ~ 270 °C, was observed (Supporting Information, Figure S6). The formation of a highly reactive peroxy radical intermediate (ROO<sup>•</sup>), then abstracting a labile hydrogen which gives rise to the hydroperoxide species (ROOH), likely occurred throughout this decomposition process in an O<sub>2</sub> environment [52]. Figure 4a also shows the thermal degradation curve of I7-(IBOMA/S)<sub>2</sub> under nitrogen atmosphere. A three-step degradation behavior was observed: a first weight loss up to about 346 °C likely due to the release of the isobornyl group [42]; a second major weight loss up to 428 °C

which may be mainly caused by the scission of isoprene-rich segments ( $T_{\text{dec,max}} = 389$  °C for the poly(isoprene) sample I4 under  $\text{N}_2$ , Figure S3b in Supporting Information); a last and minor decomposition step afterwards which might be due to the scission of the rigid IBOMA/S backbone. These three degradation steps are more distinctive when I7-(IBOMA/S)<sub>2</sub> is heated under air (Figure S6 in Supporting Information).

Thermal characterization of block copolymers is commonly used to discriminate between homogeneous and phase-separated systems. The existence of two glass transitions is then taken as evidence for a phase-separated state [53]. DSC measurements were carried out for the samples S-I4-S and I7-(IBOMA/S)<sub>2</sub> (Figure 4b). A subzero  $T_g < -62$  °C corresponding to the glass transition temperature of the flexible PI mid-block was clearly detected for both triblock copolymers.  $T_g$ s from  $-70.5$  to  $-64.5$  °C were reported for well-defined 1,4-rich PIs prepared anionically ( $\bar{D} \leq 1.22$ ) [40]. At higher temperatures,  $T_g \sim 102$  °C was determined for S-I4-S and corresponded to the glass transition temperature of the rigid PS blocks. It can be noted that the  $T_g$ s of the synthesized S-I4-S sample are very similar to those of the respective PI ( $T_{g,I4} = -60.3$  °C, Figure S3a in Supporting Information) and PS ( $T_g \sim 107$  °C for atactic PS exhibiting  $M_n = 150$  kg.mol<sup>-1</sup> [41]) homopolymers, suggesting a strong heterogeneity of the micro-structure. Regarding I7-(IBOMA/S)<sub>2</sub>, the  $T_g$  of the IBOMA-rich segments was detected at  $+182$  °C (Figure 4b). It is consistent with the literature reporting  $T_{g,P(\text{IBOMA})} = 174\text{--}206$  °C depending on the chain tacticity [54]. The relatively low  $T_g$  of the I7-(IBOMA/S)<sub>2</sub> rigid segments herein may thus be caused by the high isotactic content of the P(IBOMA) sequences. A decrease of this upper  $T_g$  may also be due to the presence of S units in the hard outer segments. Generally, the  $T_g$  of these IBOMA-rich segments is much higher than that of the PS hard blocks, reflecting the reduced chain flexibility of I7-(IBOMA/S)<sub>2</sub> due to the steric hindrance of the large isobornyl side groups.

The viscoelastic behavior of S-I4-S in the rubbery region was investigated (Figure 5). The storage modulus  $G'$  stayed relatively constant up to  $90$  °C, at which point the PS phase softened. A drastic drop of  $G'$  was observed at  $T \sim T_{g,\text{PS}} = 102$  °C (Figure 4a) since the block copolymer chains were no longer locked into position and all the chains were free to flow. The triblock copolymer I7-(IBOMA/S)<sub>2</sub> was also subjected to dynamic mechanical analysis (Figure 5). The similar  $G'$  values obtained in the rubbery plateau for I7-(IBOMA/S)<sub>2</sub> and S-I4-S can be first noted. It confirms that the glassy end-blocks do not participate to the elasticity of the copolymer. I7-(IBOMA/S)<sub>2</sub> exhibited a  $G' > 70$  MPa from room temperature to about  $150$  °C. In comparison, an analogous triblock copolymer composed of a flexible poly( $\beta$ -myrcene) mid-segment and two IBOMA-rich outer segments (IBOMA-My-IBOMA type copolymer,  $M_n = 94.7$  kg.mol<sup>-1</sup>,  $\bar{D} = 2.23$ ,  $F_{My} = 0.59$ ), synthesized by SG1-based NMP, showed a much lower  $G' = 2\text{--}13$  MPa in the rubbery plateau [29]. The relatively high storage modulus observed at  $T < T_{g,\text{hard block}}$  for the isoprene-based triblock copolymers highlights the presence of a more entangled elastomeric continuous phase compared to My-based polymers [30]. The softening of the IBOMA-rich segments of I7-(IBOMA/S)<sub>2</sub> was evidenced by the drop in  $G'$ , starting at  $155\text{--}160$  °C. The maximum value of the damping factor appeared at  $185$  °C, which is consistent with the I7-(IBOMA/S)<sub>2</sub> upper  $T_g$  measured previously via DSC ( $182$  °C, Figure 4b). Generally, the DMA test suggested an attractively high service temperature for this IBOMA-I-IBOMA type triblock.

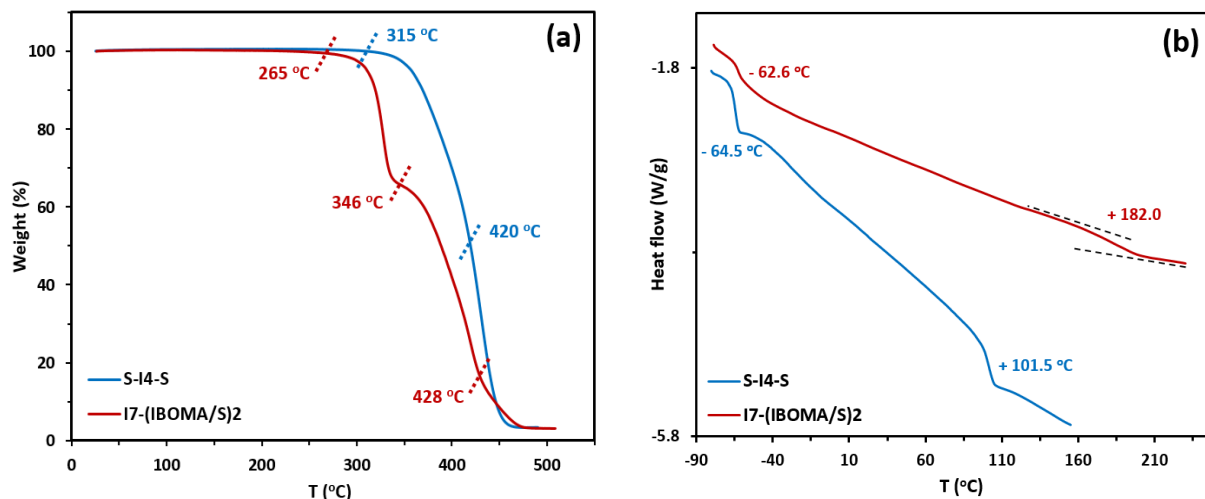


**Figure 4.** (a) TGA traces ( $10\text{ }^{\circ}\text{C}\cdot\text{min}^{-1}$ ) of final dry S-I4-S and I7-(IBOMA/S)<sub>2</sub> triblock copolymers under N<sub>2</sub> atmosphere. The characteristic temperatures  $T_{\text{dec},1} = 265\text{-}315\text{ }^{\circ}\text{C}$  (onset of decomposition),  $T_{\text{dec},2} = 346\text{-}428\text{ }^{\circ}\text{C}$  (temperatures between two degradation steps for I7-(IBOMA/S)<sub>2</sub>) and  $T_{\text{dec,max}} = 420\text{ }^{\circ}\text{C}$  (temperature at which weight loss is most apparent for S-I4-S) were determined. (b) DSC traces (second heating run) of final dry S-I4-S and I7-(IBOMA/S)<sub>2</sub> samples. The numbers near the changes in slope correspond to the  $T_{\text{g}}$ s determined via the inflection method. (1-column fitting image, top-down organization for (a) and (b))

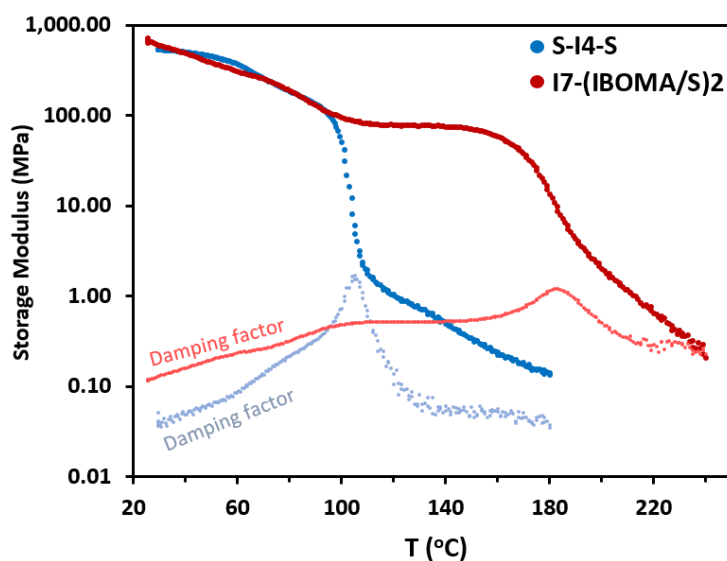


**Figure 5.** Dynamic mechanical analysis of the samples S-I4-S and I7-(IBOMA/S)<sub>2</sub> by torsional oscillation, yielding the storage modulus *versus* temperature (0.15 Hz, 1% strain, 5 °C.min<sup>-1</sup>, N<sub>2</sub> atmosphere, samples prepared by dichloromethane casting). The damping factor *versus* temperature is also shown for S-I4-S (blue) and I7-(IBOMA/S)<sub>2</sub> (red). (1-column fitting image)

Atomic force microscopy (AFM):

Atomic force microscopy was applied to study the surface morphology of S-I5-S ( $F_S = 0.30$ ,  $M_{n,GPC} = 94.6K$ ,  $\bar{D} = 2.29$ , Table 2C) in order to know if the two component blocks exhibited micro-phase separation. Figure 6 shows a 2  $\mu\text{m}$  x 2  $\mu\text{m}$  scan of the surface morphology of S-I5-S. A clear phase separation was observed with the dark area (76%, as determined by ImageJ software application, binary mode) corresponding to the continuous PI domain whereas the light area (24%) corresponded to the discrete PS phase. The solubility parameters for isoprene ( $\delta_I = 15.3 \text{ MPa}^{1/2}$ ) and styrene ( $\delta_S = 19.1 \text{ MPa}^{1/2}$ ) were calculated using the Hansen solubility parameters (HSP) [55]. This difference in  $\delta$  supports the immiscibility between the PI and PS blocks. The domain structure might be cylindrical (disordered cylinder phases), although a definite assignment requires further study. Despite a relatively low PS content (30 mol%) in this triblock copolymer, a lamellar microstructure may be suggested, as notably supported by a few examples in the literature [56,57]. The potential lamellae/cylinders observed in Figure 6 exhibited a width of  $38.5 \pm 19.1 \text{ nm}$  (NanoScope Analysis, section command). It may be argued that the apparent disorganization of these lamellae/cylinders is due to the high dispersity of the sample S-I5-S ( $\bar{D} = 2.29$ ). Several studies, based on phase-separated block copolymer blends and systems with unimodal molar mass distributions, reported an increase in domain size, lattice spacing and interfacial thickness with  $\bar{D}$ , due to changes in entropy [58]. However, it cannot be claimed that narrow molecular weight distributions are required for block copolymers to self-assemble into ordered morphologies. For instance, PS-*b*-PAA (PAA = poly(acrylic acid)) diblock copolymers ( $\bar{D} = 2.10\text{-}2.61$ ,  $F_S = 0.34\text{-}0.77$ ), synthesized by RDRP, formed well-ordered meso-structures, typically observed for nearly mono-disperse block copolymers [59].

The morphology of I7-(IBOMA/S)<sub>2</sub> was visualized by atomic force microscopy (AFM) as well.  $\delta_{1,4\text{-PI}} = 16.7 \text{ MPa}^{1/2}$ ,  $\delta_{PS} = 24.2 \text{ MPa}^{1/2}$  and  $\delta_{P(\text{IBOMA})} = 21.8 \text{ MPa}^{1/2}$  were calculated using the component group distribution method of Hoftyzer and Van Krevelen (Supporting Information, page S10) since HSP values are not given in the literature for IBOMA [60]. Figure 6 presents a representative AFM phase trace of this triblock copolymer, and an unusual organization of the two phases at the micro-scale was observed. I7-(IBOMA/S)<sub>2</sub> having  $F_1 = 0.59$ , the brighter domain (74% as determined via ImageJ) can be assigned to the continuous PI matrix. It can be hypothesized that the elastomeric PI domain, trapped between rigid IBOMA/S disperse phases, tended to protrude out from the surface. These possible PI protrusions appeared as maximums/peaks in the 3D topography image (Figure S8 in Supporting Information, same region) of I7-(IBOMA/S)<sub>2</sub>. Generally, this AFM study did not allow to distinctly determine a morphology (weakly aligned cylinders/lamellae might be present) and this system could be qualified as poorly ordered.

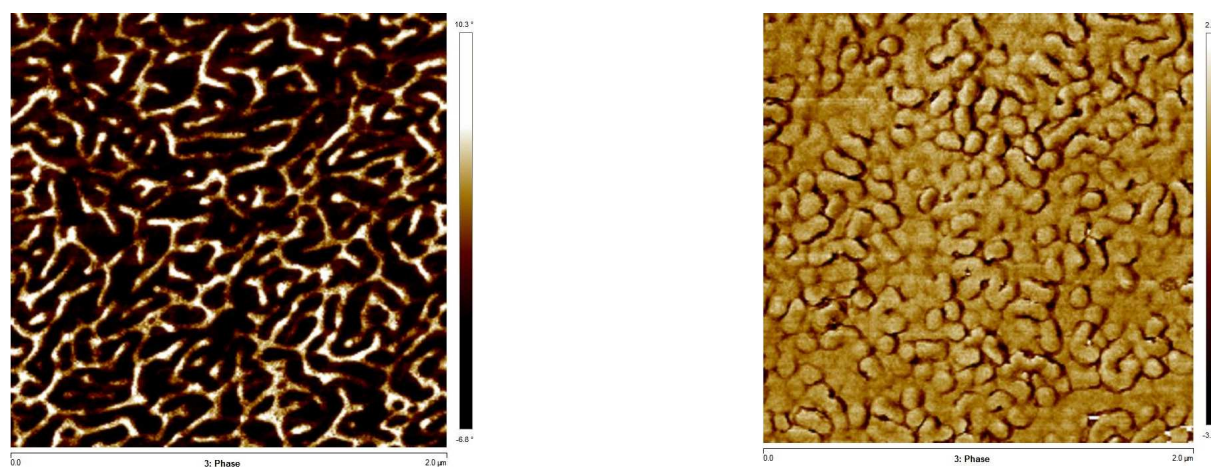


**Figure 6.** Atomic force microscopy (AFM, experimental section) phase images (2  $\mu\text{m}$  x 2  $\mu\text{m}$ ) under tapping mode of operation of the surface morphology of triblock copolymer **S-I5-S** cast film (**left**

**image**, the dark domain represents the isoprene component) and triblock copolymer **I7-(IBOMA/S)<sub>2</sub>** cast film (**right image**, the light domain represents the isoprene component). The color-coded height scale is given to the right of each image. (1-column fitting image, top-down organization for the 2 images)

#### Tensile testing:

The tensile stress-strain plots of the synthesized S-I-S polymers are presented in Figure 7a-c. As expected, tensile stress at break  $\sigma_B$  increased and elongation at break  $\varepsilon_B$  decreased as  $F_S$  increased. S-I5-S ( $F_S = 0.30$ ) and S-I6-S ( $F_S = 0.38$ ) can be considered as flexible materials with a relatively high irreversible extensibility ( $\varepsilon_B \sim 375$ -450 %, Figures 7a and 7b). These two triblocks exhibited a tensile yield strength at low elongation (10-60 %) followed by a significant plastic region. Although  $\sigma_B$  slightly increased during the plastic deformation, no strain hardening was observed for these samples, limiting thus their tensile strength at break. Such a stress-strain behavior may be explained by their possible disorganized cylindrical/lamellar micro-structure, not allowing a large-scale orientation and alignment of the macromolecules in the direction of the load. It may be assumed that a S-I-S sample exhibiting a spherical morphology (hard blocks forming discrete minority spheres embedded in a rubbery matrix) would have favored the strain hardening due to its isotropic nature. A hard and brittle S-I4-S was characterized with  $\sigma_B = 10.8 \pm 1.2$  MPa and  $\varepsilon_B = 21 \pm 7$  % (Figure 7c) due to its high styrene content ( $F_S = 0.49$ ).

Tensile testing at room temperature for I7-(IBOMA/S)<sub>2</sub> was also performed to highlight the influence of the hard segments' nature. The stress-strain curves of four I7-(IBOMA/S)<sub>2</sub> dog-bone specimens are given in Figure 7d. The limit of elastic behavior was marked by a yield point at 20-30% elongation. It was followed by a non-reversible plastic deformation until the specimen failure at  $\varepsilon_B = 1356 \pm 214$  %. Such a high stretch capacity is comparable to commercial diene/styrene thermoplastic elastomers. Interestingly, a reduced extensibility was observed for S-I-S samples previously synthesized (Figures 7a and 7b) with  $\varepsilon_B \leq 450\%$ , while they possessed a similar PI mid-segment ( $M_{n,GPC} \sim 52$ -59K,  $\bar{D} = 1.46$ -1.59, Table 2A). Accordingly, it might be due to the PS outer segments of the S-I-S materials not being able to withstand mechanical stress at high elongation unlike the IBOMA-rich blocks of I7-(IBOMA/S)<sub>2</sub>. Furthermore, this latter sample exhibited a tensile strength at break,  $\sigma_B = 11.4 \pm 0.6$  MPa, higher than those of the S-I-S samples having  $F_S \leq 0.38$  ( $\sigma_B \leq 4.1$  MPa, Figures 7a and 7b), stressing the beneficial combination of an entangled PI matrix with very rigid IBOMA-rich phases. A higher tensile stress is typically observed for styrenic thermoplastic elastomers, when replacing PS hard blocks by higher  $T_g$  blocks. Fetters and Morton obtained stress-strain data for S-I-S and MS-I-MS triblocks (MS =  $\alpha$ -methylstyrene), synthesized using 1,4-dilithio-1,1,4,4-tetraphenylbutane as the initiator and having the same average chain length ( $M_n = 127$  kg.mol<sup>-1</sup>) and an equivalent hard block / soft block ratio ( $F_1 = 0.67$ -0.69) [61]. MS-I-MS block copolymer ( $T_{g,P(MS)} \sim 173$  °C) exhibited a markedly higher tensile strength than that of S-I-S in low-strain and high-strain regions. The effects of the elastomer mid-segment type can also be observed by comparing I7-(IBOMA/S)<sub>2</sub> with the IBOMA-*M<sub>y</sub>*-IBOMA type triblock copolymer ( $F_{M_y} = 0.59$ ,  $M_n = 94.7$  kg.mol<sup>-1</sup>,  $\bar{D} = 2.23$ ) previously prepared by NMP in a similar way [29]. While the *M<sub>y</sub>*-based copolymer exhibited  $\sigma_B = 3.90 \pm 0.22$  MPa and  $\varepsilon_B = 490 \pm 31\%$ ,  $\sigma_B$  and  $\varepsilon_B$  almost tripled when substituting the *cis*-1,4-rich P(*M<sub>y</sub>*) mid-block by a *cis*-1,4-rich PI mid-block. This is likely due to the soft PI domain of I7-(IBOMA/S)<sub>2</sub>, being much more entangled ( $M_{n,PI} = 52.1K \sim 10M_{e,PI}$  with  $M_{e,PI} = 4$ -6 kg.mol<sup>-1</sup>, the entanglement molar mass of PI) than the flexible P(*M<sub>y</sub>*) matrix ( $M_{n,P(M_y)} = 51.7$  kg.mol<sup>-1</sup>  $\sim 2M_{e,P(M_y)}$  with  $M_{e,P(M_y)} = 22$ -31 kg.mol<sup>-1</sup>) of the IBOMA-*M<sub>y</sub>*-IBOMA copolymers [30].

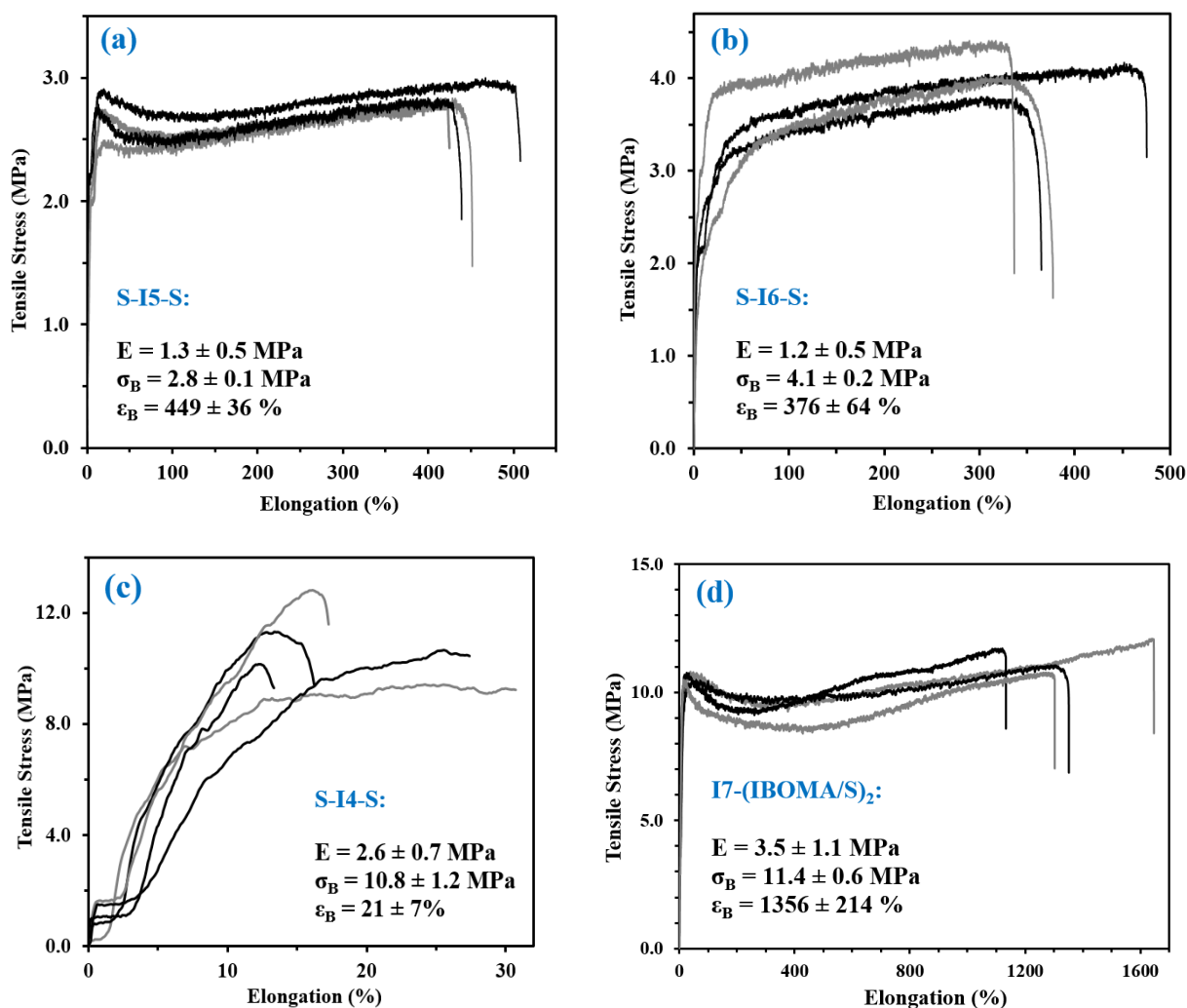


**Figure 7.** Uniaxial tensile stress-strain curves at room temperature and a cross-head speed of  $15 \text{ mm}\cdot\text{min}^{-1}$  of (a) four S-I5-S specimens ( $F_S = 0.30$ ), (b) four S-I6-S specimens ( $F_S = 0.38$ ), (c) five S-I4-S specimens ( $F_S = 0.49$ ) and (d) four I7-(IBOMA/S)<sub>2</sub> specimens, all prepared via a film casting process from dichloromethane solution. The average Young's modulus  $E$ , tensile stress at break  $\sigma_B$  and tensile elongation at break  $\epsilon_B$  obtained from these curves are also given. (2-column fitting image)

## Conclusion

The NMP of isoprene was performed at  $115^\circ\text{C}$  in pyridine using poly(ethylene-*ran*-butylene) difunctional initiator, terminated with SG1 nitroxide groups. Telechelic *cis*-1,4-rich PI-(SG1)<sub>2</sub> ( $M_{n,\text{GPC}} = 52\text{-}59\text{K}$ ,  $\mathcal{D} = 1.46\text{-}1.59$ ) were obtained and showed a good ability to re-initiate at  $115^\circ\text{C}$  fresh batches of S in bulk and a IBOMA/S mixture (91/9 mol%) in toluene.

Depending on their styrene content, the resulting S-I-S triblock copolymers ( $M_{n,\text{GPC}} = 95\text{-}109\text{K}$ ,  $\mathcal{D} = 2.11\text{-}2.29$ ) showed either a hard and brittle behavior ( $F_S = 0.49$  with  $\sigma_B \sim 11$  MPa and  $\epsilon_B \sim 20\%$ ) or a more ductile behavior ( $F_S = 0.30\text{-}0.38$  with  $\sigma_B \sim 3\text{-}4$  MPa and  $\epsilon_B \sim 375\text{-}450$  %). A micro-phase separation with the potential presence of cylinders/lamellae was observed by AFM for a S-I-S exhibiting  $F_S = 0.30$ . Due to the high  $T_g$  of its rigid blocks ( $\sim 182^\circ\text{C}$ ), the IBOMA-I-IBOMA type

triblock copolymer ( $M_{n,GPC} = 94K$ ,  $\mathcal{D} = 1.76$ ,  $F_1 = 0.59$ ) maintained an elevated storage modulus ( $G' > 55$  MPa) up to 160 °C. Moreover, its significant toughness and high extensibility were determined via tensile tests ( $\sigma_B \sim 11.4$  MPa and  $\varepsilon_B \sim 1350\%$ ) at room temperature. Generally, strengthening during large strain deformation of these triblock copolymers was not observed, which may be due to their broad molecular weight distributions and/or their elevated hard block content.

This study can pave the way to the preparation by NMP of diene-based triblock copolymers exhibiting properties similar to those of styrenic thermoplastic elastomers. Improvements can be implemented such as the synthesis of the flexible mid-block macro-initiator in a dispersed medium. For instance, the preparation by mini-emulsion of a nitroxide-terminated poly(diene), exhibiting high  $M_n > 60$  kg.mol<sup>-1</sup> and  $\mathcal{D} < 1.3$  by taking advantage of the compartmentalization effects, could be considered to produce subsequently block copolymers exhibiting a well-ordered two-phase system at the nanoscale.

### Data availability

The raw data required to reproduce these findings are available from the corresponding authors upon request.

### CRedit authorship contribution statement

**Adrien Métafiot:** Conceptualization, Methodology, Investigation, Writing - original draft. **Sébastien Pruvost:** Investigation. **Jean-Francois Gérard:** Supervision, Writing – review & editing. **Brigitte Defoort:** Supervision, Funding acquisition. **Milan Maric:** Supervision, Conceptualization, Writing – review & editing.

### Declaration of Competing Interest

The authors declare that they have no known competing financial interests or personal relationships that could have appeared to influence the work reported in this paper.

### Acknowledgements

ArianeGroup and the French Defense Procurement Agency (Direction Générale de l'Armement, DGA) supported this work financially. We would like to thank the Association Nationale de la Recherche et de la Technologie (ANRT) for its financial contribution. We also thank Stephen Carson of Arkema for their aid in obtaining the BlocBuilder™ alkoxyamine initiator used in this work.

### References:

- [1] J.G. Drobny, Chapter 1 - Introduction, in: J.G. Drobny (Ed.), Handbook of Thermoplastic Elastomers (2<sup>nd</sup> Ed.), Andrew Inc., Norwich, 2014, 1-11. <https://doi.org/10.1016/B978-0-323-22136-8.00001-6>
- [2] H.L. Hsieh, R.C. Farrar, Polymers, rubbers, synthetic (block copolymers), in: J.J. McKetta, W. A. Cunningham (Eds.), Encyclopedia of Chemical Processing and Design, Marcel Dekker Inc., New York, 1992, pp 32-66.
- [3] G. Theodosopoulos, M. Pitsikalis, Block copolymers by anionic polymerization: recent synthetic routes and developments, in: N. Hadjichristidis, A. Hirao (Eds.), Anionic Polymerization: Principles, Practice, Strength, Consequences and Applications, Springer, Tokyo, 2015, pp 541-550. [https://doi.org/10.1007/978-4-431-54186-8\\_12](https://doi.org/10.1007/978-4-431-54186-8_12)
- [4] H.L. Hsieh, R.P. Quirk, Commercial applications of anionically prepared polymers, in: H.L. Hsieh, R.P. Quirk (Eds.), Anionic polymerization: principle and practical applications, CRC Press, Boca Raton, 1996, pp 475-532. <https://doi.org/10.1201/9780585139401>
- [5] F. Wenger, Effects of impurities on the control of anionic batch polymerizations, J. Polym. Sci. 60 (1962) 99-111. <https://doi.org/10.1002/pol.1962.1206017004>
- [6] K. Ratkanthwar, N. Hadjichristidis, J.W. Mays, High vacuum techniques for anionic polymerization, in: N. Hadjichristidis, A. Hirao (Eds.), Anionic Polymerization: Principles, Practice, Strength, Consequences and Applications, Springer, Tokyo, 2015, pp 19-60. [https://doi.org/10.1007/978-4-431-54186-8\\_2](https://doi.org/10.1007/978-4-431-54186-8_2)

- [7] K. Ratkanthwar, J. Zhao, H. Zhang, N. Hadjichristidis, J.W. Mays, Schlenk techniques for anionic polymerization, in: N. Hadjichristidis, A. Hirao (Eds.), *Anionic Polymerization: Principles, Practice, Strength, Consequences and Applications*, Springer, Tokyo, 2015, pp 3-18. [https://doi.org/10.1007/978-4-431-54186-8\\_1](https://doi.org/10.1007/978-4-431-54186-8_1)
- [8] J. Chiefari, Y. Chong, F. Ercole, J. Krstina, J. Jeffery, T. Le, R. Mayadunne, G. Meijs, C. Moad, G. Moad, E. Rizzardo, S. Thang, Living free-radical polymerization by reversible addition-fragmentation chain transfer: The RAFT process, *Macromolecules* 31 (1998) 5559–5562. <https://doi.org/10.1021/ma9804951>
- [9] W.A. Braunecker, K. Matyjaszewski, Controlled/living radical polymerization: Features, developments, and perspectives, *Prog. Polym. Sci.* 32 (2007) 93–146. <https://doi.org/10.1016/j.progpolymsci.2006.11.002>
- [10] M.K. Georges, R.P.N. Veregin, P.M. Kazmaier, G.K. Hamer, Narrow molecular weight resins by a free-radical polymerization process, *Macromolecules* 26 (1993) 2987–2988. <https://doi.org/10.1021/ma00063a054>
- [11] R.P.N. Veregin, M.K. Georges, P.M. Kazmaier, G.K. Hamer, Free radical polymerizations for narrow polydispersity resins: electron spin resonance studies of the kinetics and mechanism, *Macromolecules* 26 (1993) 5316–5320. <https://doi.org/10.1021/ma00072a007>
- [12] J.-S. Wang, K. Matyjaszewski, Controlled/"living" radical polymerization. atom transfer radical polymerization in the presence of transition-metal complexes, *J. Am. Chem. Soc.* 117 (1995) 5614–5615. <https://doi.org/10.1021/ja00125a035>
- [13] D.H. Solomon, E. Rizzardo, P. Cacioli, Polymerization process and polymers produced thereby, US Patent 4581429 A, Commonwealth Scientific and Industrial Research Organization, 1986. <https://www.lens.org/lens/patent/102-999-753-817-037>
- [14] J. Nicolas, Y. Guillaneuf, C. Lefay, D. Bertin, D. Gimes, B. Charleux, Nitroxide-mediated polymerization, *Prog. Polym. Sci.* 38 (2013) 63–235. <https://doi.org/10.1016/j.progpolymsci.2012.06.002>
- [15] F. Chauvin, P.E. Dufils, D. Gimes, Y. Guillaneuf, S.R. Marque, P. Tordo, D. Bertin, Nitroxide-mediated polymerization: The pivotal role of the  $k_d$  value of the initiating alkoxyamine and the importance of the experimental conditions, *Macromolecules* 39 (2006) 5238-5250. <https://doi.org/10.1021/ma0527193>
- [16] J. Nicolas, B. Charleux, O. Guerret, S. Magnet, Nitroxide-mediated controlled free-radical emulsion polymerization of styrene and n-butyl acrylate with a water-soluble alkoxyamine as initiator, *Angew. Chem. Int. Ed.* 43 (2004) 6186-6189. <https://doi.org/10.1002/anie.200460704>
- [17] J.L. Pradel, B. Ameduri, B. Boutevin, Use of controlled radical polymerization of butadiene with AIBN and TEMPO for the determination of the NMR characteristics of hydroxymethyl groups, *Macromol. Chem. Phys.* 200 (1999) 2304–2308. [https://doi.org/10.1002/\(SICI\)1521-3935\(19991001\)200:10%3C2304::AID-MACP2304%3E3.0.CO;2-6](https://doi.org/10.1002/(SICI)1521-3935(19991001)200:10%3C2304::AID-MACP2304%3E3.0.CO;2-6)
- [18] J.L. Pradel, B. Ameduri, B. Boutevin, Controlled radical polymerization of 1,3-butadiene. II. Initiation by hydrogen peroxide and reversible termination by TEMPO, *J. Polym. Sci., Part A: Polym. Chem.* 38 (2000) 3293–3302. [https://doi.org/10.1002/1099-0518\(20000915\)38:18%3C3293::AID-POLA80%3E3.0.CO;2-0](https://doi.org/10.1002/1099-0518(20000915)38:18%3C3293::AID-POLA80%3E3.0.CO;2-0)
- [19] B. Keoshkerian, M. Georges, M. Quinlan, R. Veregin, B. Goodbrand, Polyacrylates and polydienes to high conversion by a stable free radical polymerization process: Use of reducing agents, *Macromolecules* 31 (1998) 7559–7561. <https://doi.org/10.1021/ma971686r>
- [20] E. Rizzardo, D. Solomon, A new method for investigating the mechanism of initiation of radical polymerization, *Polym. Bull.* 1 (1979) 529-534. <https://doi.org/10.1007/BF00254480>
- [21] D. Benoit, E. Harth, P. Fox, R.M. Waymouth, C.J. Hawker, Accurate structural control and block formation in the living polymerization of 1,3-dienes by nitroxide-mediated procedures, *Macromolecules* 33 (2000) 363–370. <https://doi.org/10.1021/ma9911871>
- [22] C. Cheng, K. Qi, E. Khoshdel, K.L. Wooley, Tandem synthesis of core–shell brush copolymers and their transformation to peripherally cross-linked and hollowed nanostructures, *J. Am. Chem. Soc.* 128 (2006) 6808–6809. <https://doi.org/10.1021/ja061892r>
- [23] J.K. Wegrzyn, T. Stephan, R. Lau, R.B. Grubbs, Preparation of poly(ethylene oxide)-block-poly(isoprene) by nitroxide mediated free radical polymerization from PEO macroinitiators, *J. Polym. Sci., Part A: Polym. Chem.* 43 (2005) 2977–2984. <https://doi.org/10.1002/pola.20756>

- [24] A. Sundararaman, T. Stephan, R.B. Grubbs, Reversible restructuring of aqueous block copolymer assemblies through stimulus induced changes in amphiphilicity, *J. Am. Chem. Soc.* 130 (2008) 12264–12265. <https://doi.org/10.1021/ja8052688>
- [25] Y. Cai, K.B. Aubrecht, R.B. Grubbs, Thermally induced changes in amphiphilicity drive reversible restructuring of assemblies of ABC triblock copolymers with statistical polyether blocks, *J. Am. Chem. Soc.* 133 (2010) 1058–1065. <https://doi.org/10.1021/ja109262h>
- [26] H. Matsuoka, Y. Suetomi, P. Kaewsaiha, K. Matsumoto, Nanostructure of a poly(acrylic acid) brush and its transition in the amphiphilic diblock copolymer monolayer on the water surface, *Langmuir* 25 (2009) 13752–13762. <https://doi.org/10.1021/la901466h>
- [27] S. Harrisson, P. Couvreur, J. Nicolas, SG1 Nitroxide-mediated polymerization of isoprene: Alkoxyamine structure/control relationship and  $\alpha,\omega$ -chain-end functionalization, *Macromolecules* 44 (2011) 9230–9238. <https://doi.org/10.1021/ma202078q>
- [28] S. Harrisson, P. Couvreur, J. Nicolas, Use of solvent effects to improve control over nitroxide-mediated polymerization of isoprene, *Macromol. Rapid Commun.* 33 (2012) 805–810. <https://doi.org/10.1002/marc.201100866>
- [29] A. Métafiot, L. Gagnon, S. Pruvost, P. Hubert, J. -F. Gerard, B. Defoort, M. Maric,  $\beta$ -Myrcene/isobornyl methacrylate SG1 nitroxide-mediated controlled radical polymerization: synthesis and characterization of gradient, diblock and triblock copolymers, *RSC Adv.* 9 (2019) 3377-3395. <https://doi.org/10.1039/C8RA09192G>
- [30] L.J. Fetters, D.J. Lohse, R.H. Colby, Chain dimensions and entanglement spacings, In: J.E. Mark (Ed.), *Physical Properties of Polymers Handbook* (2<sup>nd</sup> Ed.), Springer, New York, 2007, pp 447-454. [https://doi.org/10.1007/978-0-387-69002-5\\_25](https://doi.org/10.1007/978-0-387-69002-5_25)
- [31] B. Lessard, C. Aumand-Bourque, R. Chaudury, D. Gomez, A. Haroon, N. Ibrahimian, S. Mackay, M.-C. Noel, R. Patel, S. Sitaram, S. Valla, B. White, M. Maric, Poly(ethylene-co-butylene)-b-(styrene-ran-maleic anhydride)<sub>2</sub> compatibilizers via nitroxide mediated radical polymerization, *Int. Polym. Process.* 26 (2011) 197–204. <https://doi.org/10.3139/217.2425>
- [32] B. Suppaibulsuk, P. Prasassarakich, G.L. Rempel, Factorial design of nanosized polyisoprene synthesis via differential microemulsion polymerization, *Polym. Adv. Technol.* 21 (2010) 467–475. <https://doi.org/10.1002/pat.1450>
- [33] H. Sato, Y. Tanaka, <sup>1</sup>H-NMR Study of polyisoprenes, *J. Polym. Sci.: Polym. Chem.* 17 (1979) 3551–3558. <https://doi.org/10.1002/pol.1979.170171113>
- [34] J. Nicolas, S. Brusseau, B. Charleux, A minimal amount of acrylonitrile turns the nitroxide-mediated polymerization of methyl methacrylate into an almost ideal controlled/living system, *J. Polym. Sci., Part A: Polym. Chem.* 48 (2010) 34-47. <https://doi.org/10.1002/pola.23749>
- [35] C. Petit, B. Luneau, E. Beaudoin, D. Gigmes, D. Bertin, Liquid chromatography at the critical conditions in pure eluent: an efficient tool for the characterization of functional polystyrenes, *J. Chromatogr. A* 1163 (2007) 128-137. <https://doi.org/10.1016/j.chroma.2007.06.039>
- [36] D. Bertin, D. Gigmes, S.R.A. Marque, P. Tordo, P. Polar, steric, and stabilization effects in alkoxyamines C-ON bond homolysis: A multiparameter analysis, *Macromolecules* 38 (2005) 2638–2650. <https://doi.org/10.1021/ma050004u>
- [37] D.R. D'Hooge, M.-F. Reyniers, G.B. Marin, The crucial role of diffusional limitations in controlled radical polymerization, *Macromol. React. Eng.* 7 (2013) 362–379. <https://doi.org/10.1002/mren.201300006>
- [38] D.R. Morey, J.W. Tamblyn, The fractional precipitation of molecular-weight species from high polymers. Theories of the process and some experimental evidence, *J. Phys. Chem.* 51 (1947) 721–746. <https://doi.org/10.1021/j150453a012>
- [39] A. Kotera, Chapter B.1 – Fractional Precipitation, in: M.J.R. Cantow (Ed.), *Polymer Fractionation*, Academic Press Inc., New York, 1967, pp. 43-66. <https://doi.org/10.1016/B978-1-4832-3245-4.50007-8>
- [40] J.M. Widmaier, G.C. Meyer, Glass transition temperature of anionic polyisoprene, *Macromolecules* 14 (1981) 450-452. <https://doi.org/10.1021/ma50003a041>
- [41] J. Rieger, The glass transition temperature of polystyrene: Results of a round robin test, *J. Therm. Anal. Calorim.* 46 (1996) 965-972. <https://doi.org/10.1007/BF01983614>

- [42] A. Matsumoto, K. Mizuta, T. Otsu, Synthesis and thermal properties of poly(cycloalkyl methacrylate)s bearing bridged- and fused-ring structures, *J. Polym. Sci., Part A: Polym. Chem.* 31 (1993) 2531–2539. <https://doi.org/10.1002/pola.1993.080311014>
- [43] W. Michaeli, A. Grefenstein, W. Frings, Synthesis of polystyrene and styrene copolymers by reactive extrusion, *Adv. Polym. Tech.* 12 (1993) 25-33. <https://doi.org/10.1002/adv.1993.060120103>
- [44] X. Yuan, Y. Guan, S. Li, A. Zheng, Anionic bulk polymerization to synthesize styrene-isoprene diblock and multiblock copolymers by reactive extrusion, *J. Appl. Polym. Sci.* 131 (2014) 39429-39438. <https://doi.org/10.1002/app.39429>
- [45] J.-M. Wang, X.-Y. Yuan, D. Shan, A. Zheng, Styrene/isoprene/styrene thermoplastic elastomer prepared by anionic bulk polymerization in a twin-screw extruder, *Int. Polym. Proc.* 30 (2015) 44-50. <https://doi.org/10.3139/217.2884>
- [46] T. Fukuda, T. Terauchi, A. Goto, K. Ohno, Y. Tsujii, T. Miyamoto, S. Kobatake, B. Yamada, Mechanisms and kinetics of nitroxide-controlled free radical polymerization, *Macromolecules* 29 (1996) 6393-6398. <https://doi.org/10.1021/ma960552v>
- [47] G. Gryn'ova, C.Y. Lin, M.L. Coote, Which side-reactions compromise nitroxide mediated polymerization? *Polym. Chem.* 4 (2013) 3744-3754. <http://xlink.rsc.org/?DOI=c3py00534h>
- [48] G. Moad, A.G. Anderson, F. Ercole, H.J. Johnson, J. Krstina, C.L. Moad, E. Rizzardo, T.H. Spurling, S.H. Thang, Controlled-growth free-radical polymerization of methacrylate esters: Reversible chain transfer versus reversible termination, *ACS Symp. Ser.* 685 (1998) 332-360. <https://doi.org/10.1021/bk-1998-0685.ch021>
- [49] C. Burguière, M. Dourges, B. Charleux, J.P. Vairon, Synthesis and characterization of  $\omega$ -unsaturated poly(styrene-*b*-*n*-butylmethacrylate) block copolymers using TEMPO-mediated controlled radical polymerization, *Macromolecules* 12 (1999) 3883-3890. <https://doi.org/10.1021/ma982037y>
- [50] B. Charleux, J. Nicolas, O. Guerret, Theoretical expression of the average activation–deactivation equilibrium constant in controlled/living free-radical copolymerization operating via reversible termination. Application to a strongly improved control in nitroxide-mediated polymerization of methyl methacrylate, *Macromolecules* 38 (2005) 5485-5492. <https://doi.org/10.1021/ma050087e>
- [51] A. Métafiot, Y. Kanawati, J.-F. Gérard, B. Defoort, M. Maric, Synthesis of  $\beta$ -myrcene-based polymers and styrene bBlock and statistical copolymers by SG1 nitroxide-mediated controlled radical polymerization, *Macromolecules* 50 (2017) 3101-3120. <https://doi.org/10.1021/acs.macromol.6b02675>
- [52] J.D. Peterson, S. Vyazovkin, C.A. Wight, Kinetics of the thermal and thermo-oxidative degradation of polystyrene, polyethylene and poly(propylene), *Macromol. Chem. Phys.* 202 (2001) 775-784. [https://doi.org/10.1002/1521-3935\(20010301\)202:6%3C775::AID-MACP775%3E3.0.CO;2-G](https://doi.org/10.1002/1521-3935(20010301)202:6%3C775::AID-MACP775%3E3.0.CO;2-G)
- [53] B. Stuhn, The relation between the microphase separation transition and the glass transition in diblock copolymers, *J. Polym. Sci., Part B: Polym. Phys.* 30 (1992) 1013-1019. <https://doi.org/10.1002/polb.1992.090300909>
- [54] J.M. Yu, P. Dubois, R. Jérôme, Poly[alkyl methacrylate-*b*-butadiene-*b*-alkyl methacrylate] triblock copolymers: Synthesis, morphology, and mechanical properties at high temperatures, *Macromolecules* 29 (1996) 8362-8370. <https://doi.org/10.1021/ma960886k>
- [55] C.M. Hansen, Chapter 1 – Solubility parameters, an introduction, in: C.M. Hansen (Ed.), *Hansen Solubility Parameters: A User's Handbook* (2<sup>nd</sup> ed.), CRC Press, New York, 2007, pp 1-26. [https://books.google.ca/books?id=gprF31cvT2oC&pg=PA1&hl=fr&source=gbg\\_toc\\_r&cad=4](https://books.google.ca/books?id=gprF31cvT2oC&pg=PA1&hl=fr&source=gbg_toc_r&cad=4)
- [56] R. van den Berg, H. de Groot, M.A. van Dijk, D.R. Denley, Atomic force microscopy of thin triblock copolymer films, *Polymer* 35 (1994) 5778-5781. [https://doi.org/10.1016/S0032-3861\(05\)80056-4](https://doi.org/10.1016/S0032-3861(05)80056-4)
- [57] A.K. Khandpur, S. Foerster, F.S. Bates, I.W. Hamley, A.J. Ryan, W. Bras, K. Almdal, K. Mortensen, Polyisoprene-polystyrene diblock copolymer phase diagram near the order-disorder transition, *Macromolecules* 28 (1995) 8796-8806. <https://doi.org/10.1021/ma00130a012>
- [58] N.A. Lynd, A.J. Meuler, M.A. Hillmyer, Polydispersity and block copolymer self-assembly, *Prog. Polym. Sci.* 33 (2008) 875-893. <https://doi.org/10.1016/j.progpolymsci.2008.07.003>
- [59] D. Bendejacq, V. Ponsinet, M. Joanicot, Y.-L. Loo, R.A. Register, Well-ordered microdomain structures in polydisperse poly(styrene)–poly(acrylic acid) diblock copolymers from controlled radical polymerization, *Macromolecules* 35 (2002) 6645–6649. <https://doi.org/10.1021/ma020158z>

- [60] D.W. van Krevelen, K. Te Nijenhuis, Chapter 7 – Cohesive Properties and Solubility, in: D.W. van Krevelen, K. Te Nijenhuis (Eds.), *Properties of Polymers* (4<sup>th</sup> ed.), Elsevier, 2009, pp. 189-227. <https://doi.org/10.1016/B978-0-08-054819-7.00007-8>
- [61] L.J. Fetters, M. Morton, Synthesis and properties of block polymers. I. Poly- $\alpha$ -methylstyrene-polyisoprene-poly- $\alpha$ -methylstyrene, *Macromolecules* 2 (1969) 453-458. <https://doi.org/10.1021/ma60011a002>

## Graphical Abstract

Synthesis of Isoprene-based Triblock Copolymers by Nitroxide-Mediated Polymerization.

